JOURNAL OF MATERIALS SCIENCE 26 (1991) 3945–3950

Deformation mechanism in αCu–Al single crystals with a spherical indentor

Part I *Indentation with steel ball*

S. KOBAYASHI
Department of Mechanical Engineering, Doshisha University, Kamigyoku, Kyoto, Japan
T. HARADA
Food Laboratory, Kanebo Co., Ltd., Kajiwara, Takatsuki, Japan
S. MIURA
Department of Engineering Science, Kyoto University, Sakyoku, Kyoto, Japan

Indentation tests using a steel ball were carried out on the (0 0 1), (0 1 1) and (1 1 1) cube faces of αCu–Al single crystals in order to elucidate the plastic deformation mechanism in the surface layers. The shapes of the indent and the slip traces produced on these faces were studied in detail. In addition, the dislocation density distributions around an indent on the (1 1 1) and ($\bar{2}$ 1 1) faces were revealed by successively removing thin layers and developing etch pits on the exposed surfaces. Slip tends to occur in the ⟨1 1 0⟩ direction on the (0 0 1) and (0 1 1) faces, and in the [2 $\bar{1}$ $\bar{1}$], [$\bar{1}$ 2 $\bar{1}$] and [$\bar{1}$ $\bar{1}$ 2] directions on the (1 1 1) face. The three-dimensional slip pattern in the case of indentation on the (1 1 1) face consists of two sets of truncated triangular pyramids that diverge and converge downwards.

1. Introduction

Abrasive wear is caused where a softer metallic material is rubbed by asperity tips of a harder material, or when wear particles produced by friction are pressed into a material. In order to clarify such wear mechanisms, it is necessary to focus on a deformation mechanism in the case where a harder asperity tip is indented into a softer material. For this purpose, it is effective to investigate the slip mechanism on a microscopic level using single crystals, because metallic materials have slip systems which vary with each material.

Although extensive studies have been made on the plastic deformation of single crystals, relatively little work has been done on plastic deformation in terms of the dislocation patterns which are associated with an indentation.

Some experimental work has been done on the dislocation patterns produced when a spherical indentor is pressed into the cube face of single crystals [1–3]. In these studies, observations were made only on the top surface deformed by an indentor. A few attempts have been made to study the subsurface deformation mechanism associated with indentation. Yoshioka *et al.* [4] have reported slip trace distribution and dislocation distribution on the cube face at various depths.

Recently, in this field of study, it has become more important to take into account the deformation pattern produced inside the material. The object of the present study was to find the actual distributions of slip traces and dislocations near to and just below a ball indent on an αCu–Al single crystal, and to explain the anisotropy of deformation.

The shape of the indent produced by a ball indentor and the associated slip trace distributions were studied in detail. In addition, the dislocation density variations near the indent on the (1 1 1) and ($\bar{2}$ 1 1) faces were revealed by successively removing thin layers and developing etch pits on the exposed surface.

2. Experimental procedure

2.1. Sample preparation

Single crystals used in this study were grown from Cu–14.7 at % Al alloys by the Bridgman technique. The specimen was prepared in a following manner. A thin parallelepiped with dimensions 8 mm × 10 mm × 15 mm was cut from the single crystal using electrical discharge machining. The orientation was chosen so that one of the long faces was parallel to a {1 1 1} face.

The specimens were sealed in an evacuated quartz tube and annealed for 50 h in the temperature range 750–950 °C. This treatment resulted in sufficient crystal perfection to permit cleavage without excessive damage.

After annealing, the crystal face of the specimen used for indentation was polished mechanically and electrolytically to remove the oxide layer and to obtain a mirror-finished surface. A polishing solution of

0022–2461/91 $03.00 + .12

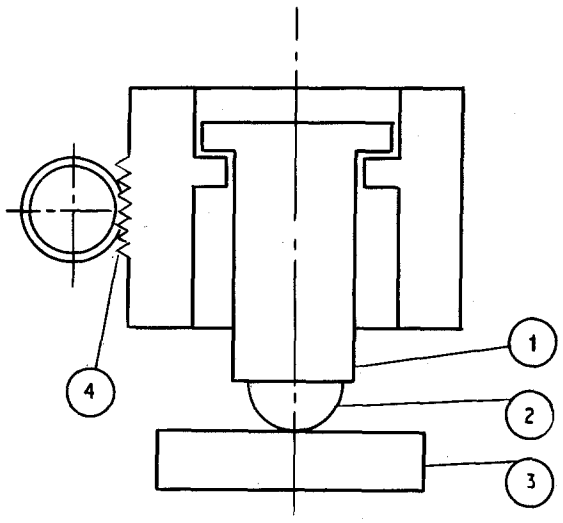

Figure 1 Loading device. (1) Weight, (2) indentor, (3) specimen, (4) rack.

25.0 vol % C_2H_5OH in concentrated H_2PO_4 was used at room temperature.

The chemical compositions of the solution used for etching are shown in Table I. It was confirmed that the dislocation density of the annealed and polished surface was reduced to 5×10^5 cm^{-2}.

2.2. Experimental details

The indentations were made at 10.0 and 1.0 N using a $\frac{1}{4}$ in. ($\sim$ 6.4 mm) diameter steel ball which had been finely ground to produce a surface finish of about 0.05 μm. The ball was mounted on a loading device as shown in Fig. 1 in such a manner that the weight (1) and a ball (2) were loaded on a specimen (3) by moving the rack (4) downwards. The (1 1 1) surface of the specimen was set exactly perpendicular to the loading axis. The load was applied for 1 min on all occasions. Care was taken to ensure that the load was applied without shock. After indentation, the shape of the indent and the slip traces around it were observed.

The specimen was then re-etched to reveal the dislocation structure resulting from indentation. The dislocation density around the indent on the (1 1 1) and ($\bar{2}$ 1 1) faces were revealed by successively removing thin layers from the surface and developing etch pits on the exposed surfaces. The thickness of each removed layer was determined both by using the weight loss method and by measuring the specimen thickness with a projecting apparatus.

TABLE I Chemical compositions of etching solution (ml.)

H_2O	HCl	CH_3COOH	Br_2
100	60	20	2

3. Results and discussion

3.1. Appearances of the (0 0 1), (0 1 1) and (1 1 1) surfaces before etching

Fig. 2 shows the characteristic pattern of an indent topography made on the (0 0 1) face of a Cu–Al crystal under a load of 10.0 N. The shape of the indent after loading is that of a rounded square whose sides are slightly drawn in. The indented region is considered to be divided into octants bounded by the ⟨1 1 0⟩ and ⟨1 0 0⟩ directions. One such divided region is outlined in Fig. 2.

The square shape of the indent indicates that the material can be deformed more easily at the ⟨1 1 0⟩ azimuths than at the ⟨1 0 0⟩ azimuths. Anisotropy in the indent shape has been reported for metals such as copper and aluminium [5]. These observed facts provide a means of determining the approximate places of dislocation origin and cessation, as well as determining the slip systems in the case of ball indentation.

The groups of slip traces intersecting each other at right angles are found to be activated inside and near to an indent. These slip traces show that the slip plane is {1 1 1} which is inclined at 54°44′ to the (0 0 1) face and has a slip direction of ⟨1 1 0⟩. Similar patterns of slip traces were observed in copper crystal by Dyer [1].

Fig. 3a shows an indent and resulting slip traces formed on the (0 1 1) crystal face. Fig. 3b shows a

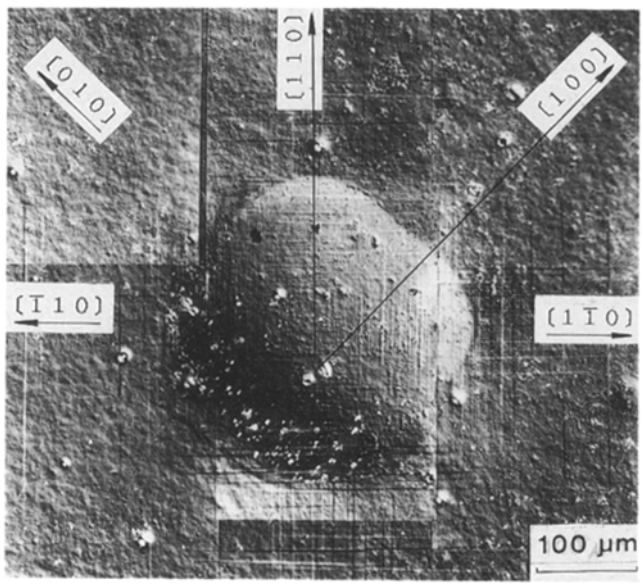

Figure 2 10.0 N indentation on (0 0 1) by 6.4 mm steel ball.

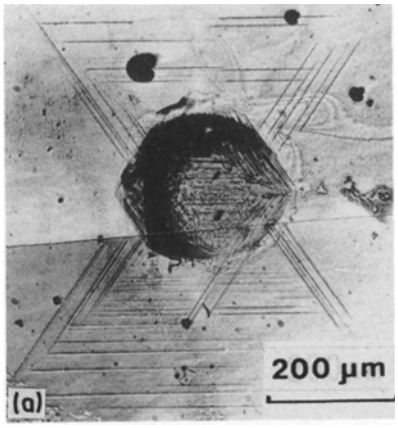

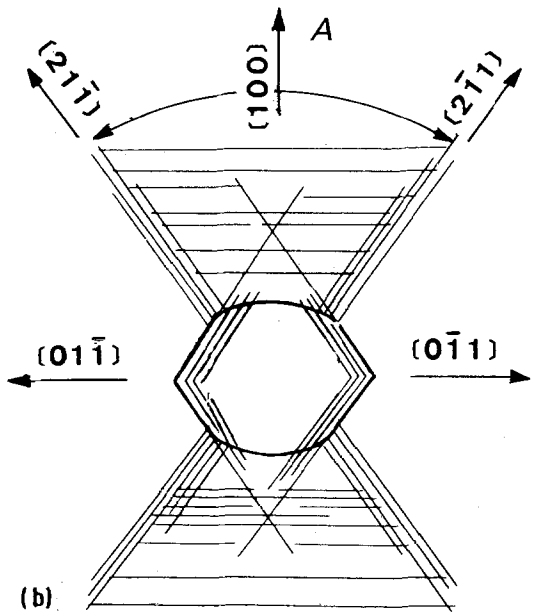

Figure 3 10.0 N indentation on (0 1 1) by 6.4 mm steel ball. (a) Deformation at surface, (b) sketch of (a).

sketch of this same indent. It was found that the indent was closer to a hexagon in shape; the anisotropy of deformation is thus more marked than on the (0 0 1) face.

In indentation tests on the (0 1 1) face, the deformation is such that theoretically eight types of slip system can operate, i.e. (1 1 1) {[1 1̄ 0], [1 0 1̄]}, (1̄ 1 1) {[1̄ 1 0], [1̄ 0 1̄]}, {(1 1 1̄), (1̄ 1 1̄)} [0 1̄ 1̄], and {(1 1̄ 1), (1̄ 1̄ 1)} [0 1̄ 1]. These families of slip traces were found to be activated in sequence as the load on the indentor was increased and were observed as two different families of slip traces.

One family consists of sets of lines parallel to the ⟨2 1 1⟩ direction and shaped like the letter "X" centring around the contact zone. At higher loads (about 2.0 N) the other family of slip traces parallel to the ⟨1 1 0⟩ direction appears, but it is located on the inner side of the X-shaped slip traces (region A, Fig. 3b).

Fig. 4 shows an indent and slip traces made at a load of 10.0 N on the (1 1 1) surface. Fig. 5a shows the etched appearance of the indent at surface level. The shape of the indent has little anisotropy and it is approximately circular in shape.

In the three shadowed portions shown in Fig. 5b, the indent became very shallow. It was found that the

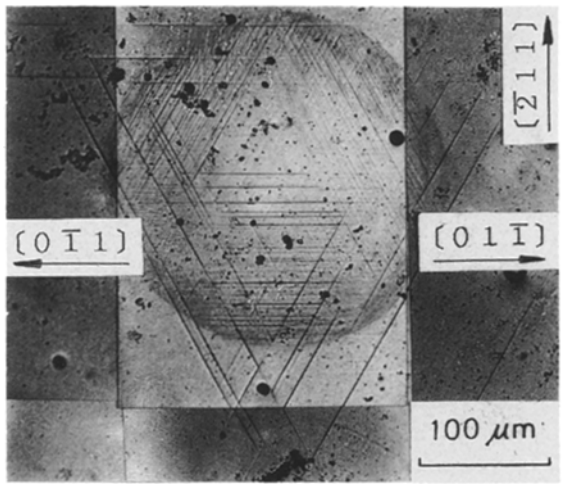

Figure 4 10.0 N indentation on (1 1 1) by 6.4 mm steel ball.

deformation was rather small in the three azimuths of [2̄ 1 1], [1 2̄ 1] and [1 1 2̄] compared with that in other azimuths.

The slip traces form triangular patterns on the inside and outside of the indent. These triangles can be divided into two distinguishable groups whose vertices point to either the [2̄ 1 1] or [2 1̄ 1̄] direction, respectively.

3.2. Deformation mechanism

Fig. 6a shows an indent on the (1 1 1) face under a load of 1.0 N. The general shape of the indent and the pattern of slip traces are similar to those in the case of the 10.0 N indentation. Fig. 6b shows the same surface after etching.

The dislocation density inside triangle ABC is estimated to be above 1×10^8 cm^{-2}, judging from the number of etch pits around the triangle. We refer to such a region as one of high dislocation density. The rows of etch pits consist of two kinds of regular triangles containing vertex points in mutually opposite directions. The dislocation patterns associated with depth levels 60, 90, 105, and 120 μm, respectively, under a 1.0 N indentation are shown in Fig. 7. Fig. 7a shows the specimen at a depth of 60 μm, where the number of etch pits is noticeably reduced. The high dislocation density region is still clearly observed at a depth of 105 μm, but it nearly disappears at that of 120 μm.

According to the results shown in Figs 6 and 7, it is clear that the sets of triangular slip traces which contain vertex points in the [2 1̄ 1̄] direction are enlarged as the depth increases. In contrast to this, triangles pointing in the opposite direction become smaller in size as the depth increases. These observations show that in the case of indentation on the (1 1 1) face, the shearing planes consist of two sets of coaxial triangular pyramids which diverge and converge downwards.

Fig. 8 shows the shear trajectories under the contact area of a rigid ball and a soft material for the elastic case. The three-dimensional case in plasticity of a ball on a flat surface has been confirmed experimentally to give similar results [6]. Shear occurs in the directions

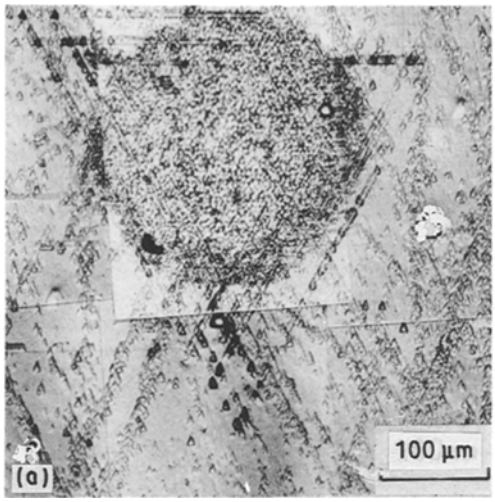

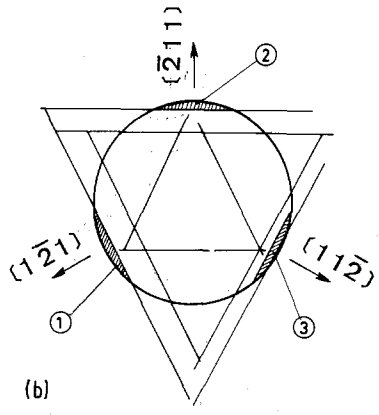

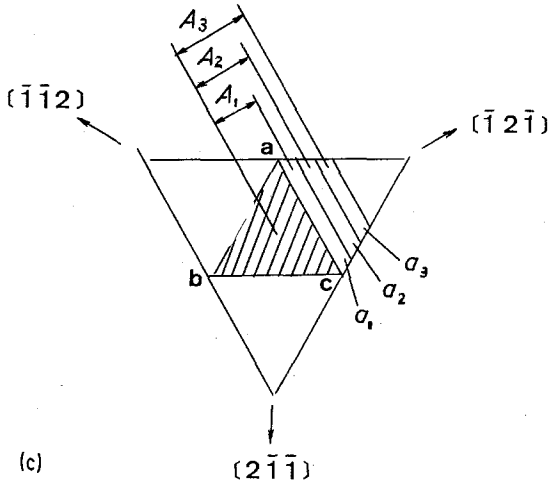

Figure 5 10.0 N indentation on (1 1 1). (a) Etched at surface level, (b) sketch of (a), (c) areas in which the number of etch pits were measured.

of the tangent to the lines drawn in Fig. 8, and once slip occurs in a given direction, it continues along the same slip vector. Therefore, on the (2̄ 1 1) face perpendicular to the (1 1 1) face, two types of slip lines which alternatingly diverge and converge downwards would be observed from the central part of an indent towards the outside as indicated in Fig. 9. The former is formed by activities of the (1̄ 1 1), (1 1̄ 1), and (1 1 1̄) planes and the latter by the (1 1̄ 1̄), (1̄ 1 1̄), and (1̄ 1̄ 1) planes. It can

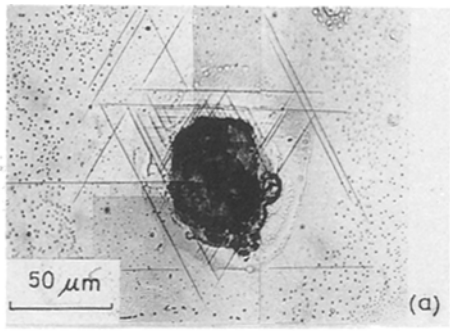

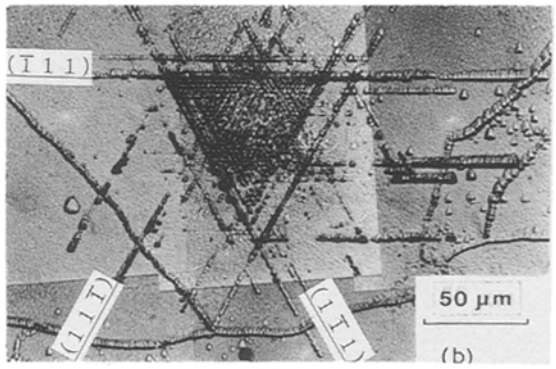

Figure 6 1.0 N indentation on (1 1 1). (a) Deformation at surface, (b) etched at surface level.

be considered that slip lines of group A accomplish the downward movement of the material under the ball and those of group B are responsible for the upward swell around the contact area.

3.3. Dislocation density associated with indentation

The dislocation densities associated with depth levels from 0.0–40 μm were examined using methods involving etch pit detection. The number of etch pits on the (1 1 1) face was counted each time a layer of 8 μm was removed by electrolytic polishing.

A calculation of etch pits per unit area was made for each trapezoidal section of 10 μm wide, a_1, a_2, a_3, . . . , around the high dislocation density region of the three azimuths [2 1̄ 1̄], [1̄ 2 1̄], and [1̄ 1̄ 2], as indicated in Fig. 5c. Relations between dislocation density and distance from the centre of the indent, A_1, A_2, A_3, . . . , were obtained on six surfaces exposed by electrolytic polishing. The results are shown in Fig. 10.

Dislocation density decreases from the high density region towards the inside, and at a distance of 130 μm, it is reduced to the value of 5×10^5 cm^{-2}, which is observed in undeformed areas. The region of high dislocation density (above 1×10^8 cm^{-2}) extends to a distance of 30 μm from the centre.

The isopleths of dislocation density on the (2̄ 1 1) face under a load of 1.0 N indentation are obtained as shown in Fig. 11. The broken line indicates where the dislocation density is equal to that before indentation. The deformation zone extends to 150 μm vertically and 125 μm horizontally from the centre of an indent. This line shows the range of plastic deformation associated with indentation.

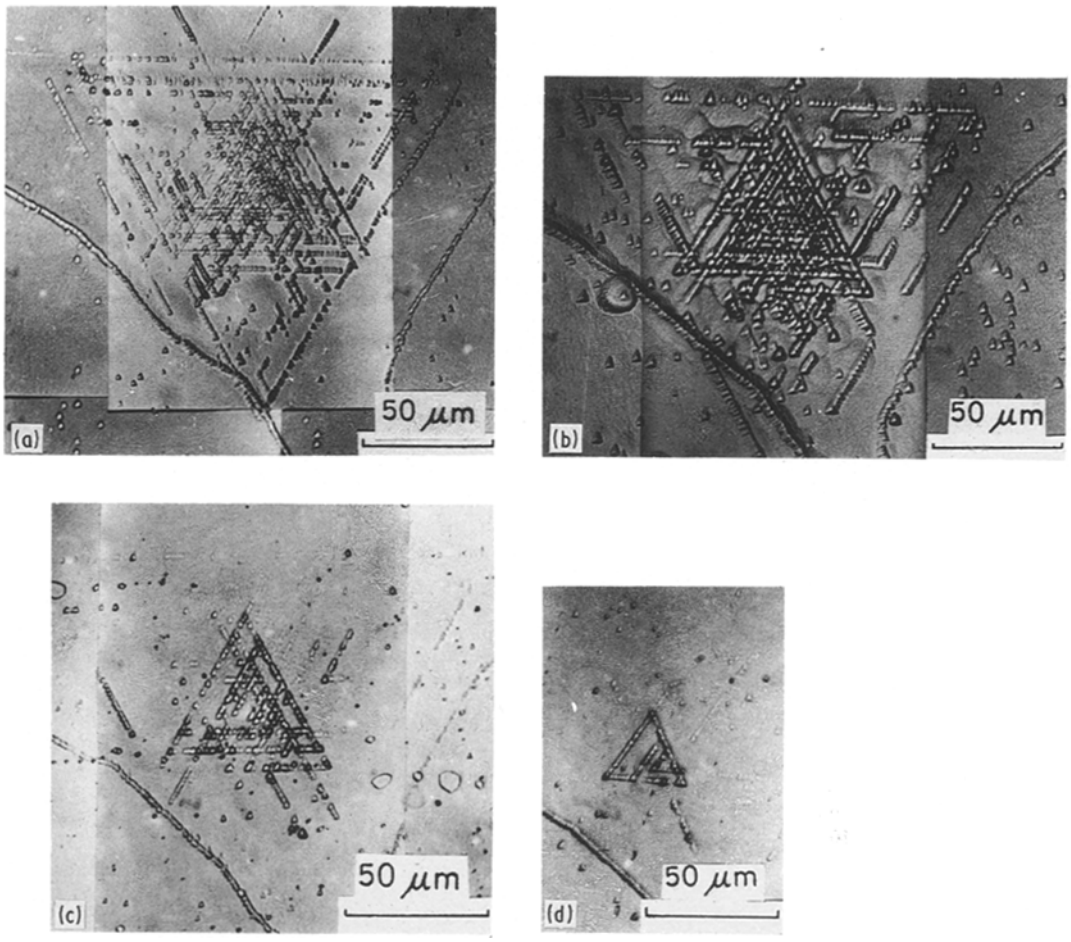

Figure 7 1.0 N indentation on (1 1 1), etched at (a) 60 μm depth, (b) 90 μm depth, (c) 105 μm depth, (d) 120 μm depth.

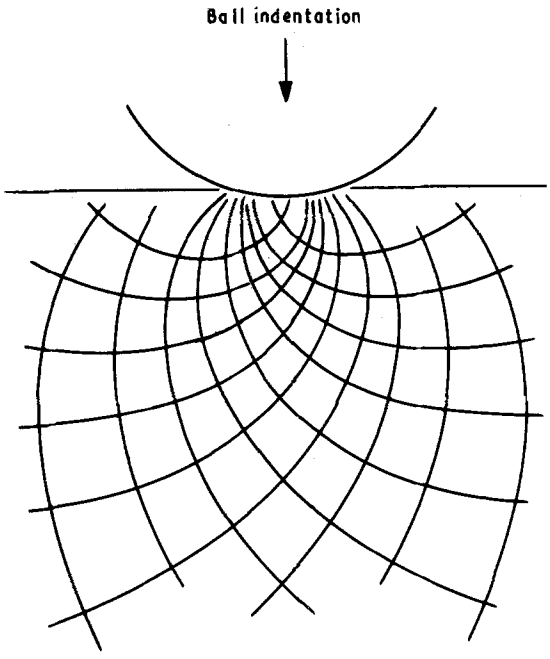

Figure 8 Shear trajectories under contact area of rigid ball.

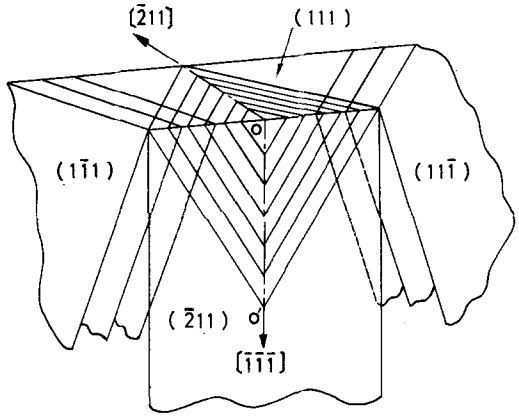

Figure 9 Preferred slip systems with ball indentation on (1 1 1).

4. Conclusions

The results of the present experiments provide further understanding about the physical appearance around an indented contact area. The main deformation mechanism for a ball pressing into the cube face of αCu–Al single crystal can be described as follows.

1. A greater degree of deformation is observed in the ⟨1 1 0⟩ azimuths compared with other azimuths on the (0 0 1) or (0 1 1) face. Deformation tends to occur in the [2 1̄ 1̄], [1̄ 2 1̄] and [1̄ 1̄ 2] azimuths on the (1 1 1) face, and it is hard to produce in the contrary azimuths on this face.

2. The three-dimensional slip pattern on the (1 1 1) face consists of an interaction of slip on two sets of planes. One set is arranged in a converging triangular

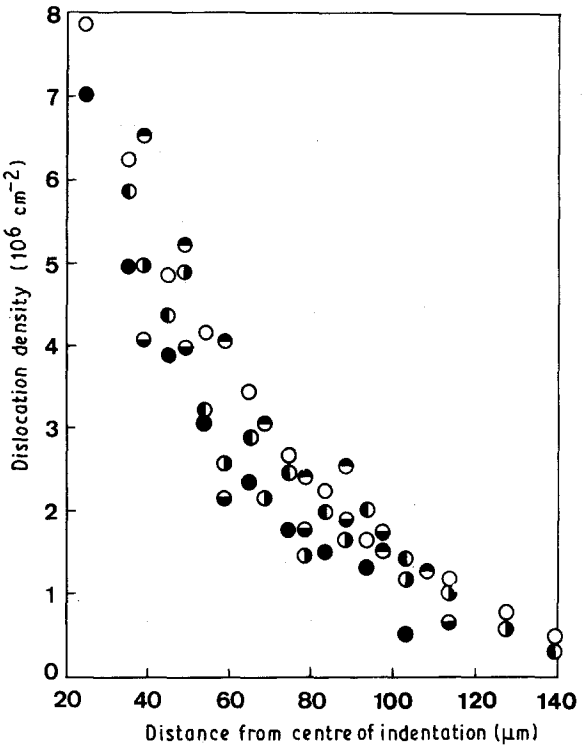

Figure 10 Dislocation density distributions under 1.0 N indentation on (1 1 1). Depth (μm): (○) 0, (◐) 8, (◓) 16, (◑) 24, (◒) 32, (●) 40.

pyramid and causes a downwards movement of the contact zone. The other set surrounds the above set with diverging pyramids, thus raising the material around the contact area.

3. The dislocation density distributions and deformation range on the (1 1 1) and ($\bar{2}$ 1 1) faces were revealed.

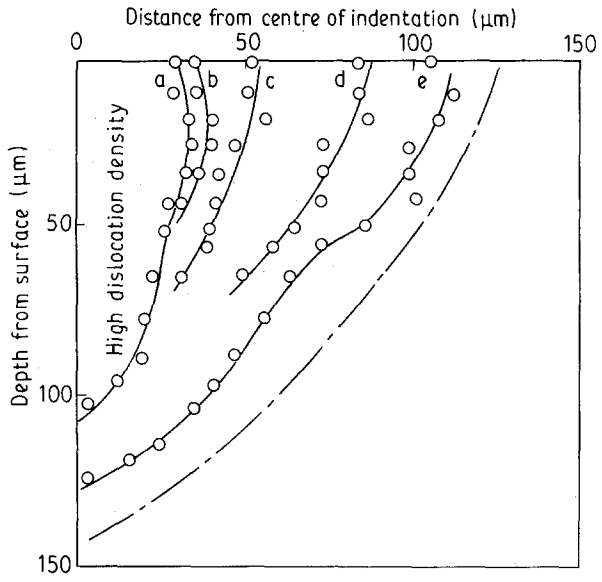

Figure 11 Isopleths of dislocation density under 1.0 N indentation on (1 1 1). Dislocation density (cm^{-3}); (a) 1×10^8, (b) 6×10^6, (c) 4×10^6, (d) 3×10^6, (e) 1×10^6, (— - —) 5×10^5.

References

1. L. D. DYER, *Trans. ASM* **50** (1965) 620.
2. A. S. KEH, *J. Appl. Phys.* **31** (1960) 1538.
3. W. RINDER and R. F. TRAMPOSCH, *ibid.* **34** (1963) 758.
4. S. YOSHIOKA, M. MAEDA and E. SUKEDAI, *J. Jpn Inst. Metals* **34** (1970) 1122.
5. M. SODA and J. SATO, *Trans. Jpn Soc. Mech. Eng.* **40** (1974) 1751.
6. R. N. HEYER, *Proc. ASTM* **37** (1937) 119.

Received 11 June
and accepted 19 November 1990